

# UniForm: A Unified Diffusion Transformer for Audio-Video Generation

Lei Zhao<sup>\*1</sup> Linfeng Feng<sup>\*1</sup> Dongxu Ge<sup>\*1</sup> Fangqiu Yi<sup>1</sup> Chi Zhang<sup>1</sup> Xiao-Lei Zhang<sup>1</sup> Xuelong Li<sup>1</sup>

## Abstract

As a natural multimodal content, audible video delivers an immersive sensory experience. Consequently, audio-video generation systems have substantial potential. However, existing diffusion-based studies mainly employ relatively independent modules for generating each modality, which lack exploration of shared-weight generative modules. This approach may under-use the intrinsic correlations between audio and visual modalities, potentially resulting in sub-optimal generation quality. To address this, we propose **UniForm**, a **unified diffusion transformer** designed to enhance cross-modal consistency. By concatenating auditory and visual information, UniForm learns to generate audio and video simultaneously within a unified latent space, facilitating the creation of high-quality and well-aligned audio-visual pairs. Extensive experiments demonstrate the superior performance of our method in joint audio-video generation, audio-guided video generation, and video-guided audio generation tasks. Our demos are available at <https://uniform-t2av.github.io/>.

## 1. Introduction

With the flourishing of deep learning, artificial intelligence generated content (AIGC) has enabled vivid creation across text (Chung et al., 2024; Li et al., 2024), images (Rombach et al., 2022; Zhu et al., 2023), audio (Liu et al., 2024a; Wang et al., 2024b), and video (Song et al., 2024; Zheng et al., 2024). It unlocks new applications in writing, design, audio, and video production, and broadens possibilities in digital media. However, AI-based content generation is typically conducted within isolated subdomains, such as text to sound effect generation (Tan et al., 2024) or text to silent video generation (Wang et al., 2024c), neglecting the integration of auditory and visual elements that are crucial for a complete immersive experience. Therefore, the aim of our current

<sup>\*</sup>Equal contribution <sup>1</sup>Institute of Artificial Intelligence (TeleAI), China Telecom. Correspondence to: Xiao-Lei Zhang <xiaolei.zhang@nwpu.edu.cn>.

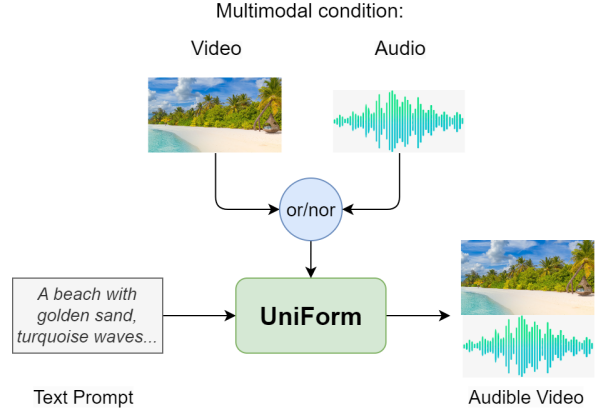


Figure 1. Illustration of multimodal-conditioned audible video generation. Video or audio can serve as a condition to guide the generation of the other; in the absence of both, audible video can be generated solely from text.

work is to generate high-quality audible video by integrating text, audio, or video inputs.

A common and straightforward approach for generating audible video content is a two-stage process: first, silent video is generated, followed by the corresponding audio based on the video. For example, in Movie Gen (Polyak et al., 2024), silent video can be generated using a single video prompt or supplemented with images as key frames. The silent video is then used as a condition in conjunction with an audio prompt to customize the audio. This approach completely decouples the generation of the two modalities. The advantage is its ease of implementation, while the drawback is that the association between audio and video may not be enough. The alignment between audio and video content faces challenges.

In contrast, recent works have focused on jointly generating audio and video. MM-Diffusion (Ruan et al., 2023) utilizes two subnets to generate audio-video pairs. In (Xing et al., 2024), a multimodal latent aligner is introduced to link powerful pre-trained single-modal generation models. They propose jointly generating video and audio using U-Net based diffusion models. In contrast, another emerging diffusion backbone is the Diffusion Transformer (DiT) (Peebles & Xie, 2023), which has demonstrated remarkable

performance in various content generation tasks. Building on this, MM-LDM (Sun et al., 2024) utilizes two separate DiTs to independently process audio and video, and enables multimodal interaction within a shared high-level semantic space finally. Similarly, (Hayakawa et al., 2024) employs two diffusion processes, followed by a joint discriminator to integrate audio and video. Meanwhile, AV-DiT (Wang et al., 2024a) adopts a shared DiT backbone pre-trained exclusively on image data, facilitating audio and video generation through the addition of lightweight adapters.

Although these methods have achieved impressive results, they typically rely on two distinct subnets to generate audio and video separately, which limits the depth of integration between these modalities. Motivated by the natural pairing of audible videos, we explored whether a unified model could enhance alignment and consistency between modalities. In this work, we introduce a novel approach that employs a single diffusion process to concurrently generate paired audio and video content. We present the **Unified Diffusion Transformer** (UniForm), a system for generating audio-video content. As illustrated in Figure 1, UniForm can create an audible video based solely on a text prompt, or it can accept silent video or audio as an additional input to generate the missing component, thereby completing the audible video. Remarkably, all three tasks can be accomplished using just one model. Our contributions can be summarized as follows:

- We employ a single diffusion framework for the synchronous generation of both audio and video content. Our UniForm concatenates vision and audio tokens, allowing them to undergo diffusion modelling together in a unified latent space, implicitly learning the correlations between the modalities.
- We have developed a multi-task model utilizing a single backbone with shared weights. By integrating task tokens to specify the target task, the model simultaneously supports three generation tasks: text-to-audible video (T2AV), audio-to-video (A2V), and video-to-audio (V2A). Additionally, for the latter two tasks, we have incorporated text prompts to enable finer-grained control, further enhancing performance.
- Experiments show that our UniForm achieves performance comparable to state-of-the-art single-task baselines, both in objective metrics and subjective auditory-visual experience. Remarkably, this performance is attained without the need for fine-tuning on specific task datasets, as the model is trained solely as a multi-task system.

## 2. Related Work

### 2.1. Video to Audio Generation

In this paper, we focus on “Foley” audio<sup>1</sup>, which refers to sound effects created and added during post-production to enhance the auditory experience of multimedia (Choi et al., 2023), such as simulating the crunch of leaves underfoot or the clinking of glass bottles. AI-based Foley generation in previous years was based on class labels (Liu et al., 2021) or text prompts (Liu et al., 2023). Building on this, recent advancements have expanded the scope of video-to-audio generation. (Du et al., 2023) requires conditional audio alongside silent video to generate multiple audio tracks, which are subsequently selected using an audio-visual synchronization model. DIFF-FOLEY (Luo et al., 2024) only requires silent video as input. It first learns aligned features through contrastive audio-visual pretraining (CAVP), followed by training a diffusion model conditioned on CAVP visual features within the spectrogram latent space. Meanwhile, FoleyCrafter (Zhang et al., 2024) introduces an optional text prompt to further enhance the granularity of audio generation. Additionally, it employs a semantic adapter and a temporal controller to improve alignment. LoVA (Cheng et al., 2024) use a DiT for V2A tasks, specifically targeting 10-second long videos. Unlike previous works that primarily rely on GANs or diffusion models, FRIEREN (Wang et al., 2024d) adopts a flow matching generative model as its backbone. To enhance temporal alignment, it leverages a non-autoregressive vector field estimator network that avoids downsampling along the temporal dimension.

### 2.2. Audio to Video Generation

Given the substantial information density of video, video-to-audio generation tasks can prioritize video as the primary input, with text serving a supplementary role. In contrast, audio-to-video generation tasks rely on audio mainly as a reference for alignment. This is because audio alone carries limited information (e.g., neither machines nor humans can easily determine whether a given audio clip corresponds to climbing stairs or tap dancing). As a result, audio to video generation typically requires texts or images to provide additional context for the video content. AADiff (Lee et al., 2023) is an early example of an audio-aligned diffusion framework that uses both text and audio as input. TPoS (Jeong et al., 2023) employs a stage-wise generation strategy: first, it generates an initial frame based on a text prompt, then adaptively modifies the generated images in response to the audio inputs. (Yariv et al., 2024) introduces a lightweight adaptor network that learns to map audio-based representations to the input format expected by an existing text-to-video generation model. Meanwhile, AVSyncD

<sup>1</sup>Youtube: The Magic of Making Sound

(Zhang et al., 2025) proposes and addresses a novel task: given an image, it uses an audio clip to animate the objects within the image accordingly.

### 3. Method

In this section, we introduce **Unified Diffusion Transformer** (UniForm) model to achieve not only text-guided audio and video mutual generation but also joint generation in a single model. We first review the preliminary knowledge of the process of generation based on diffusion in section 3.1.1 as well as Diffusion Transformer (DiT) model in section 3.1.2. Then in 3.1.3 we give the problem definition of our three basic generation tasks. Finally, in Section 3.2, we provide a detailed introduction to our proposed UniForm. UniForm leverages the cross-modal representation capability of DiT to successfully tackle three tasks simultaneously.

#### 3.1. Preliminaries

##### 3.1.1. DIFFUSION-BASED GENERATION

As a probabilistic generative model, diffusion model has garnered significant attention in recent years, owing to its exceptional performance in tasks like image generation (Ramesh et al., 2022) and audio generation (Liu et al., 2024a). The core idea of the diffusion model is that it first defines a process of gradually transforming a data distribution into a Gaussian noise distribution (forward process), which can be seen as a series of steps that gradually add noise. Subsequently, the model learns how to perform the inverse operation of this process, starting from pure noise and gradually denoising through a series of inverse steps, ultimately generating samples that are close to the original data distribution (reverse process).

Most existing diffusion models are built upon Denoising Diffusion Probabilistic Models (DDPMs) (Ho et al., 2020). DDPMs define the forward process as a transition from the data distribution  $X$  to the standard Gaussian distribution  $\mathcal{N}(0, \mathbf{I})$  by gradually adding noise to the original data sample  $x_0$  within discrete time step  $t$  in forward process. The forward process is defined as a Markovian process, which can be formulated as  $q(x_t | x_{t-1}) = \mathcal{N}(x_t; (1 - \beta_t)x_{t-1}, \beta_t \mathbf{I})$ , where  $x_0 \sim q(x_0)$  represents the initial true data distribution, noising schedules  $\{\beta_1, \beta_2, \dots, \beta_t, \dots, \beta_T\}$  are added over a total diffusion steps  $T$ . Re-parameterization of the forward process can be denoted as  $q(x_t | x_0) = \mathcal{N}(x_t; \bar{\alpha}_t x_0, (1 - \bar{\alpha}_t) \mathbf{I})$  where  $x_t$  represents as a direct sample from  $x_0$ ,  $\bar{\alpha}_t = \prod_{i=1}^t (1 - \beta_i)$ . This formula indicates that  $x_t$  at any timestep can be generated directly from  $x_0$  and standard Gaussian noise,  $x_t = \bar{\alpha}_t x_0 + (1 - \bar{\alpha}_t) \epsilon$ ,  $\epsilon \sim \mathcal{N}(0, \mathbf{I})$ .

The goal of the reverse process is to progressively generate  $x_0$  from pure noise  $x_T \sim \mathcal{N}(0, I)$ . Similar to for-

ward process, reverse process can also be represented as a Markov process, denoising network  $\theta$  can be formulated as  $p_\theta(x_{t-1} | x_t) = \mathcal{N}(x_{t-1}; \mu_\theta(x_t, t), \sigma_\theta^2 \mathbf{I})$ . For optimizing network  $\theta$ , we maximize the variational lower bound of the log-likelihood which equivalent to minimizing the loss  $\mathcal{L}_\theta = \sum_{t=1}^T D_{KL}(q(x_{t-1} | x_t, x_0) || p_\theta(x_{t-1} | x_t)) - \log p_\theta(x_T)$ . In practical optimization, the noise prediction loss  $\mathcal{L}_\theta$  can be simplified as minimizing a mean square loss between the denoising network prediction and ground truth added noise in forward process, defined as follows:  $\min_\theta \mathcal{L}_{simple} = \min_\theta \mathbb{E}_{x_t, t, \epsilon} \|\epsilon - \epsilon_\theta(x_t, t)\|_2^2$ . Starting from a standard Gaussian distribution  $x_T \sim \mathcal{N}(0, I)$ , the generated data  $x_0$  can be obtained by progressively sample through  $p_\theta(x_{t-1} | x_t)$ .

##### 3.1.2. DIFFUSION TRANSFORMER (DiT)

Latent Diffusion Model (LDM) (Rombach et al., 2022) transfers the diffusion process from a high-dimensional data space to a low-dimensional latent space, significantly decreasing computational overhead. LDM utilizes pre-trained autoencoders to project data into the latent space, where it subsequently performs the diffusion process using diffusers, typically a U-Net architecture (Ronneberger et al., 2015). Diffusion Transformer (DiT) (Peebles & Xie, 2023) builds upon Vision Transformer (ViT) (Dosovitskiy, 2020), serving as an enhancement to the traditional U-Net backbone for class-conditioned image generation. The self-attention mechanism of the Transformer excels at modeling global dependencies and spatial context information, making it particularly suitable for high-resolution images. In this work, we utilize DiT as the backbone of our multi-task model.

##### 3.1.3. PROBLEM DEFINITION

Our goal is to showcase that both video and audio modalities can be produced using a completely same model. This contrasts with current approaches to audio and video generation, which typically involve separate models or designs for generating video and audio. Here, we define three multi-modal generation tasks, including text to audio and video (T2AV), audio to video (A2V) and video to audio (V2A). In T2AV inference stage, given vision and audio Gaussian noise  $z_T^v$  and  $z_T^a$ , denoising network  $\theta_{av}$  aims to gradually generate two modalities simultaneously conditioned on given text. In single modality tasks A2V and V2A, diffusion model tries to generate video and audio respectively based on known modality and text description. We further employ the classifier-free guidance (CFG) scheme to enable text-conditioned generation. We train our diffusion model to predict conditional noise  $\epsilon_\theta(x_t, t, c)$  using conditional information  $c$  while predict unconditional noise  $\epsilon_\theta(x_t, t, \phi)$  when condition information is randomly drop.

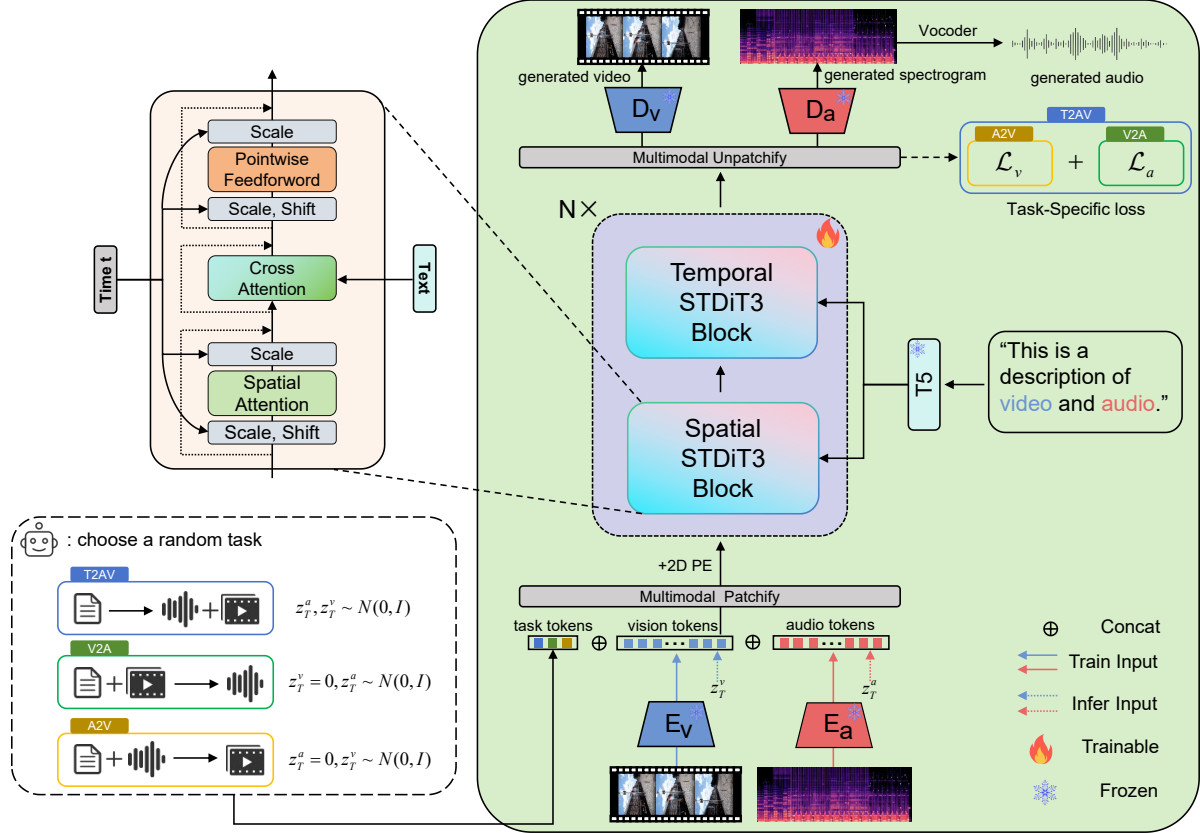


Figure 2. Overview of the proposed UniForm. Vision tokens and audio tokens are integrated and processed within a unified latent space using a DiT model to learn their representations. During training, one of three tasks is randomly selected in each iteration, with task tokens guiding the learning of the DiT. The text encoder, the encoder-decoder for video and audio, and the audio vocoder are all pre-trained models that remain frozen throughout.

### 3.2. Text-guided UniForm for Multitask Generation

To achieve free multimodal generation of audio and video within a fully unified framework. We propose a diffusion based generation framework UniForm that processes vision and audio latent in a unified space. Detailed descriptions of the key components design of our model are provided in the following part.

#### 3.2.1. VIDEO & AUDIO LATENT ENCODING

As mentioned in Section 3.1.2, DiT maps the input to the latent space in order to decrease computational costs. Our UniForm similarly follows this paradigm. More specifically, in training stage, given a batch size  $B$  input videos  $V \in \mathbb{R}^{B \times F \times C^v \times H \times W}$ , where  $F$  denotes the number of frames in the videos, each frame has  $C$  channels, with a height of  $H$  and a width of  $W$ . A 3D-VAE encoder (Zheng et al., 2024)  $E_v$  is adopted to extract vision latent  $z^v \in \mathbb{R}^{B \times \hat{C}^v \times \hat{F} \times \hat{H} \times \hat{W}}$  from videos, where  $\hat{C}^v, \hat{F}, \hat{H}, \hat{W}$  are hidden dims of vision tokens. For the audio inputs, we initially utilize the Short-Time Fourier Transform (STFT)

to convert the audio from the time domain to the frequency domain. Following this, applying a set of Mel-scale filters produces  $B$  number of 2D mel spectrograms with a shape of  $\mathbb{R}^{B \times T \times F^a}$ . Then the mel spectrogram is also extracted by a pre-trained audio VAE encoder  $E_a$  to obtain audio latent tokens  $z^a$  with a dim  $\mathbb{R}^{B \times \hat{C}^a \times \hat{F}^a \times \hat{N}}$ .

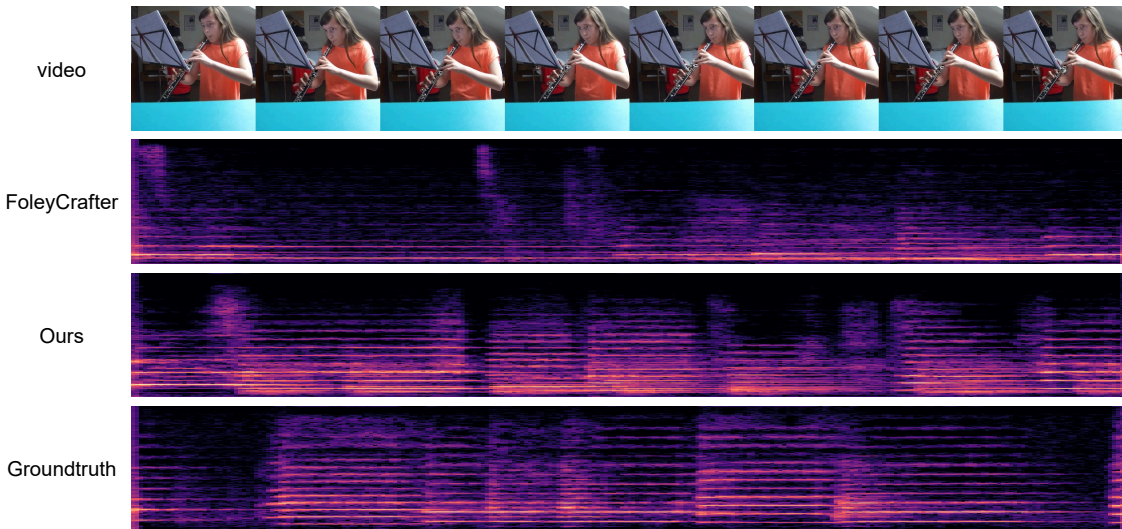
#### 3.2.2. MULTITASK EMBEDDING

As shown in Figure 2, we incorporate additional task tokens into the input to assist the model in better understanding the task. Specifically, the task ID among three tasks is passed through an Embedding layer to obtain its latent representation, which is called task token. All latent tokens remain consistent across all dimensions except for the last, which is adjusted through reshaping, and they are then connected together using concatenation. Subsequently, the input passes through a Multimodal Patch Embedder and is augmented with 2D positional encoding. Additionally, a Time Embedder is utilized to integrate time information into the input. After obtaining the joint representation of vision as well as audio as input, we adopt spatial and temporal STDiT3



Caption: The video is a dynamic scene of a white car in motion on a winding road. The car is captured in the foreground, with its headlights illuminating the path ahead. The road is flanked by lush greenery, with trees and bushes on both sides, creating a natural corridor. The car is moving at a high speed, as indicated by the blurred background and the motion blur on the car itself. The road curves gently to the right, and the car is leaning into the turn, suggesting a high-speed maneuver. The style of the image is realistic, capturing the motion and speed of the car in a natural setting.

Figure 3. An example of generated captions.



The video shows a young girl playing a flute. She is seated at a desk with a music stand in front of her, which has a sheet of music on it. The girl is wearing an orange shirt and appears to be focused on her performance. In the background, there is another person who seems to be playing a piano, as indicated by the presence of a piano keyboard and a person's hands on it. The setting appears to be an indoor space with a ceiling and a wall with a poster on it. The lighting is bright, and the overall atmosphere is calm and studious.

Text

Figure 4. Compared with FoleyCrafter in V2A generation on VGGSound dataset. Our method can generate more accurate prosody and richer high-frequency details.

(Zheng et al., 2024) Blocks to progressively integrate information from both spatial and temporal domains. In order to integrate textual information, cross attention mechanism is applied in both STDiT3 Blocks, which can be seen in Figure 2. Noted that due to spatial limitations, we only presented the spatial version of STDiT3. The temporal version of STDiT3, on the other hand, replaced the spatial attention mechanism within the module with a temporal attention mechanism, while keeping all other settings consistent.

### 3.2.3. VIDEO & AUDIO LATENT DECODING

Once we obtain the final output from the DiT blocks, we utilize Multimodal unpatchify to derive the predicted noise and variance for both the video and audio, which serves the diffusion objective. Specifically, after the diffusion process is completed, the two sampled Gaussian noises are concatenated and fed into the trained model. This process gradually reduces the noise, ultimately generating latent information with minimal noise in the final diffusion time step. The

latent representation is then divided and reconfigured into two distinct modal latent forms, corresponding to the video and audio inputs. Using the pre-trained decoder of VAEs, the latent features of both video and audio are simultaneously reconstructed into generated video frames and audio Mel-spectrograms. Subsequently, these Mel-spectrograms are further converted into audio waveforms using the pre-trained HiFi-GAN (Kong et al., 2020).

### 3.2.4. VIDEO & AUDIO GENERATION LOSS

Here, we outline the objective of our model in the denoising process for the three tasks that we previously proposed. During V2A task, the audio generation loss  $\mathcal{L}_a$  can be formulated as:

$$\mathcal{L}_a = MSE(\text{Mask}_a(\epsilon) - \text{Mask}_a(\epsilon_\theta(z_t^a, z_t^v, t, c))), \quad (1)$$

where  $\text{Mask}_a$  represents the masking operation to all latent representations, with the exception of audio tokens, i.e., task tokens, and vision tokens. For the video generation loss  $\mathcal{L}_v$

Table 1. Comparison of different methods for V2A task

Video to Audio Generation (V2A)						
Dataset	Method	Use Text?	FAD↓	FD↓	IS↑	KL↓
VGGSound	SpecVQGAN (Iashin & Rahtu, 2021)	✗	5.42	31.69	5.23	3.37
	Diff-Foley (Luo et al., 2024)	✗	4.72	23.94	11.11	3.38
	V-AURA (Viertola et al., 2024)	✗	2.88	14.80	10.08	2.42
	Seeing&Hearing (Xing et al., 2024)	✓	5.40	24.58	8.58	2.26
	VATT (Liu et al., 2024b)	✓	2.77	10.63	11.90	<b>1.48</b>
	FoleyCrafter (Zhang et al., 2024)	✓	2.51	16.24	<b>15.68</b>	2.30
	Ours	✓	<b>1.3</b>	<b>6.21</b>	14.68	2.66

Table 2. Comparison of different methods for A2V task

Audio to Video Generation (A2V)					
Dataset	Method	FVD↓	IS↑	AV-Align↑	
Landscape	MM-Diffusion (Ruan et al., 2023)	922	2.85	0.41	
	TempoToken (Yariv et al., 2024)	784	4.49	<b>0.54</b>	
	Sound-guided Video Generation (Lee et al., 2022)	544	1.16	-	
	TPoS (Jeong et al., 2023)	421	1.49	-	
	Ours	<b>319</b>	<b>4.61</b>	0.51	

in A2V task, it similarly can be denoted as:

$$\mathcal{L}_v = MSE(Mask_v(\epsilon) - Mask_v(\epsilon_\theta(z_t^a, z_t^v, t, c))), \quad (2)$$

where  $Mask_v$  also represents masking all latent representations except for vision tokens. As for the T2AV task, the multimodal loss  $\mathcal{L}_{av}$  is defined as

$$\mathcal{L}_{av} = MSE(Mask_{av}(\epsilon) - Mask_{av}(\epsilon_\theta(z_t^a, z_t^v, t, c))), \quad (3)$$

where  $Mask_{av}$  denotes only masking on task tokens. Thus  $\mathcal{L}_{av}$  is also equal to  $\mathcal{L}_a + \mathcal{L}_v$ . Note that for all three tasks, we utilize classifier-free guidance (CFG) scheme, which randomly discards text guidance with a 50% chance. This approach ensures that our model can sustain its generation performance even without a provided video (or audio) description. The model’s generation capabilities in various scenarios will be explored in subsequent sections.

## 4. Experiments

### 4.1. Experimental Setup

**Datasets:** The training datasets used in this work include AudioSet-balanced (Gemmeke et al., 2017) AudioSet-strong (Hershey et al., 2021), VGGSound (Chen et al., 2020) and Landscape (Lee et al., 2022). AudioSet is a large-scale Audio-visual dataset released by Google, which contains more than a million labeled video clips extracted from YouTube videos. Each clip has been manually annotated, marking one or more sound events present within it. AudioSet-balanced consists of 22,176 segments selected

from the AudioSet, with each class having at least 59 samples. AudioSet-strong involves selecting approximately 67,000 segments from AudioSet and annotating them at the frame level (with a resolution of 0.1 seconds), resulting in corresponding strong labels. VGGSound is an extensive single-label audio-visual dataset comprising more than 200,000 videos. Landscape is a high-fidelity dataset that encompasses video and audio streams, highlighting nine varied natural scenes, including but not limited to raining, splashing water, thunder, and underwater bubbling.

**Implementation:** For data preprocessing, we resample the videos to 17 fps and then resize them to a resolution of  $256 \times 256$ , and we resample the audios at 16 kHz. Then, we truncate the first 4s of the video and audio samples as the input for VAEs. The pre-trained VAEs from Open-Sora (Zheng et al., 2024) and AudioLDM (Liu et al., 2023) are used to encode/decode videos and audios, respectively. We adopt pllava (Xu et al., 2024) to generate video captions, in the format illustrated in Figure 3. As for the Landscape dataset, we use its class labels as captions. Our DiT model utilizes pre-trained weights from image generation (Chen et al., 2024). We set the batch size to 32 and conducted 1000 epochs of iterations with a constant learning rate of  $1 \times 10^{-4}$  using the HybridAdam optimizer. Linear warmup is adopted as the learning rate scheduling strategy, and the warmup step is set to 1000.

**Evaluation metrics:** For evaluating video generation, we adopt the Fréchet Video Distance (FVD), Kernel Video Distance (KVD) and Inception Score (IS). We adhered to

Table 3. Comparison of different methods for T2AV task

Joint Video and Audio Generation (T2AV)					
Dataset	Method	FVD↓	KVD↓	FAD↓	AV-Align↑
Landscape	Seeing&Hearing (Xing et al., 2024)	1175	34.8	6.46	0.28
	MM-Diffusion (Ruan et al., 2023)	447	-	5.78	0.24
	Discriminator-guided Diffusion (Hayakawa et al., 2024)	405	-	<b>5.52</b>	0.24
	Ours	<b>326</b>	<b>22.8</b>	5.61	<b>0.30</b>

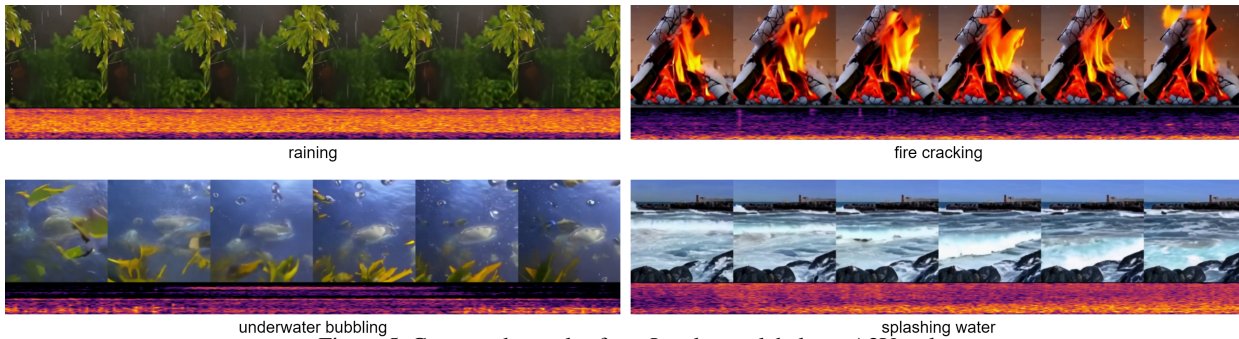


Figure 5. Generated samples from Landscape labels on A2V task

the setting described in (Hayakawa et al., 2024) for the training split of the landscape dataset. For audio generation, our evaluation relies on the metrics Frechet Audio Distance (FAD), Frechet Distance (FD), kullback-leibler divergence (KL) and IS. Additionally, we utilize the AV-align (Xing et al., 2024) metric to assess the synchronization between generated audio and video.

#### 4.2. Results on Video to Audio Generation

Table 1 lists the comparison results of our multi-task model with some recent approaches on video to audio generation. From the table, we can see that our method outperforms the majority of baselines across most metrics. Specifically, it achieves first place in both the FAD (1.3) and FD (6.21) metrics, leading over FoleyCrafter (Zhang et al., 2024) and VATT (Liu et al., 2024b), which are ranked second in those respective categories with FAD scores of 2.51 and 2.77, and FD scores of 16.24 and 10.63, respectively. Additionally, our model secures second place in the IS metric with a score of 14.68, closely following FoleyCrafter (Zhang et al., 2024), which ranks first with an IS score of 15.68. Notably, with the exception of (Xing et al., 2024), the other baseline methods are restricted to single video-to-audio tasks. This highlights that our multi-task model can generate audio that is highly relevant to the video content, with a quality that rivals the best current V2A approaches.

Figure 4 presents a visual comparison between the mel spectrograms of the audio generated by our method and that produced by FoleyCrafter (Zhang et al., 2024). Compared to FoleyCrafter, our method exhibits higher visual correlation

with the ground truth, especially noticeable in the first half of the mel spectrogram where FoleyCrafter lacks certain elements. Additionally, our approach captures more high-frequency details.

#### 4.3. Results on Audio to Video Generation

Table 2 highlights the exceptional performance of our method in audio-to-video generation. Specifically, our approach achieves the lowest FVD score (319), demonstrating its ability to generate videos with the highest quality. Meanwhile, in terms of IS, which measures content diversity, our approach also leads (4.61), showcasing its strength in generating varied content. Although our method’s AV-Align score (0.51) is slightly lower than that of TempoToken (0.54), overall, our method excels in the field of audio-to-video generation, particularly in video quality and diversity. This highlights our method’s ability to enhance synchronization between audio and visual elements while significantly improving the overall quality of generated videos. Figure 5 showcases four exemplary generations by our method using class labels of Landscape dataset.

#### 4.4. Results on Joint Audio-Video Generation

Table 3 lists the comparison results of different methods for joint video and audio generation on the Landscape dataset. As shown in the table, our method performs excellently on the FVD (326), KVD (22.8), and AV-Align (0.30) metrics, indicating that the generated video content is not only more realistic but also better aligned between audio and video. Our model is somewhat less competitive on the audio genera-

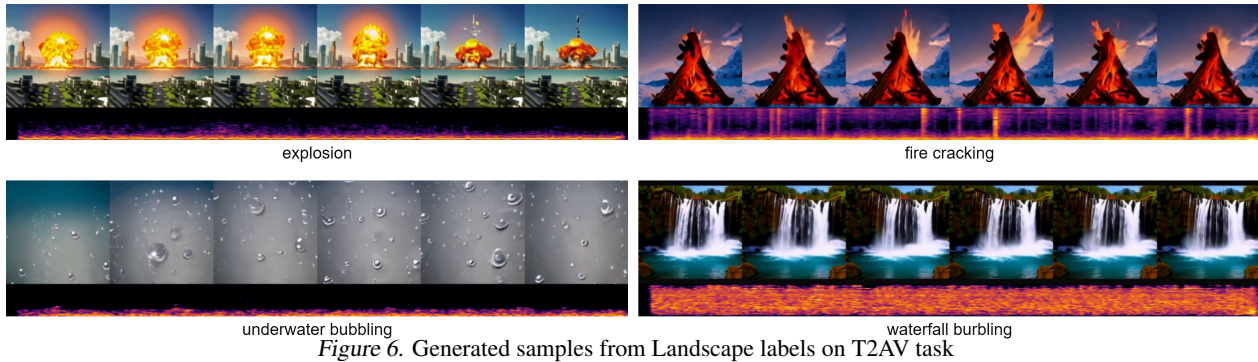
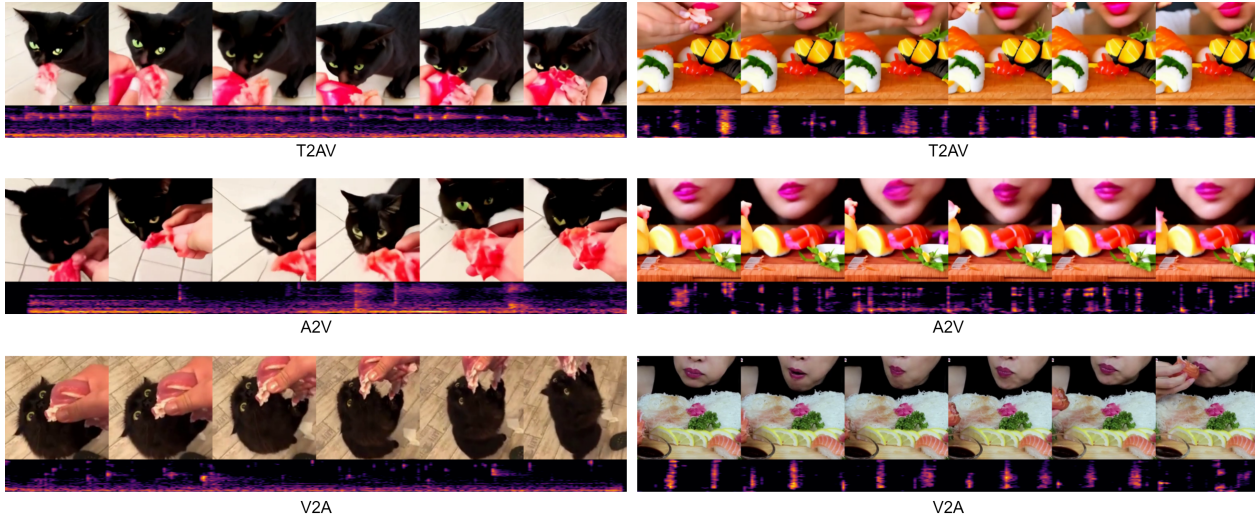


Figure 6. Generated samples from Landscape labels on T2AV task



The video shows a black cat with striking green eyes being fed a piece of pink meat by a person's hand. The cat is sitting on a tiled floor, and the person's hand is holding the meat close to the cat's mouth. The cat appears to be in a state of anticipation or curiosity, with its mouth open and eyes focused on the meat. The person's hand is visible, with a nail polish on the thumb. The image is a close-up shot, capturing the interaction between the cat and the meat.

The video is a close-up shot of a person's face, likely a woman, with a pouty expression and a hint of lipstick. She is holding a piece of sushi in her hand, which appears to be a salmon nigiri, and is about to take a bite. The sushi is garnished with a pink flower and a sprig of greenery. In the foreground, there is a wooden cutting board with various sushi pieces, including slices of lemon, arranged neatly. The background is blurred, but it seems to be an indoor setting with a warm, ambient lighting.

Figure 7. Generated two challenging samples on VGGSound dataset

tion metric FAD, with a score of 5.61, falling slightly behind the Discriminator-Guided Diffusion approach (Hayakawa et al., 2024), which achieves an FAD score of 5.52. Figure 6 showcases some generation examples of our method using Landscape labels.

Figure 7 displays two challenging generation examples on three tasks, both involving live subjects with detailed movements. As can be seen, our generated examples exhibit high video generation quality and coherence. Using the ground truth as baseline, our method demonstrates high consistency in both video and audio under text guidance. These improvements are features that many previous T2AV generation methods lacked, as they were only trained on toy datasets.

#### 4.5. Ablations on text prompts

Table 4 demonstrates the influence of text on both V2A and A2V tasks. Clearly, employing text as a conditional guide markedly improves the quality of generated videos

and audios, a fact that is consistently reflected across all metrics in both tasks.

Table 4. The influence of text on V2A and A2V tasks

TASK	Use text?	FAD↓	FD↓	IS↑	KL↓
V2A	✗	2.39	9.96	7.06	3.14
	✓	<b>1.3</b>	<b>6.21</b>	<b>14.68</b>	<b>2.66</b>
		FVD↓	IS↑	AV-align↑	
A2V	✗	319	2.91	0.32	
	✓	<b>521</b>	<b>4.61</b>	<b>0.51</b>	

## 5. Conclusions

We have introduced a novel unified audio-video generation model, UniForm, which achieves simultaneous audio and video synthesis using a single diffusion framework. Built on a diffusion transformer (DiT) backbone, it employs distinct task tokens to enable audio-video synthesis under



varying conditions. Our approach enhances both the generation quality of audio and video and their multimodal alignment. UniForm achieves state-of-the-art generation quality, as demonstrated by subjective perception and objective metric evaluations. This performance is attained without the need for task-specific fine-tuning.

## References

- Chen, H., Xie, W., Vedaldi, A., and Zisserman, A. Vgsgound: A large-scale audio-visual dataset. In *ICASSP 2020-2020 IEEE International Conference on Acoustics, Speech and Signal Processing (ICASSP)*, pp. 721–725. IEEE, 2020.
- Chen, J., Wu, Y., Luo, S., Xie, E., Paul, S., Luo, P., Zhao, H., and Li, Z. Pixart- $\delta$ : Fast and controllable image generation with latent consistency models. *arXiv preprint arXiv:2401.05252*, 2024.
- Cheng, X., Wang, X., Wu, Y., Wang, Y., and Song, R. Lova: Long-form video-to-audio generation. *arXiv preprint arXiv:2409.15157*, 2024.
- Choi, K., Im, J., Heller, L., McFee, B., Imoto, K., Okamoto, Y., Lagrange, M., and Takamichi, S. Foley sound synthesis at the dcase 2023 challenge. In *arXiv e-prints: 2304.12521*, 2023.
- Chung, H. W., Hou, L., Longpre, S., Zoph, B., Tay, Y., Fedus, W., Li, Y., Wang, X., Dehghani, M., Brahma, S., et al. Scaling instruction-finetuned language models. *Journal of Machine Learning Research*, 25(70):1–53, 2024.
- Dosovitskiy, A. An image is worth 16x16 words: Transformers for image recognition at scale. *arXiv preprint arXiv:2010.11929*, 2020.
- Du, Y., Chen, Z., Salamon, J., Russell, B., and Owens, A. Conditional generation of audio from video via foley analogies. In *Proceedings of the IEEE/CVF Conference on Computer Vision and Pattern Recognition*, pp. 2426–2436, 2023.
- Gemmeke, J. F., Ellis, D. P., Freedman, D., Jansen, A., Lawrence, W., Moore, R. C., Plakal, M., and Ritter, M. Audio set: An ontology and human-labeled dataset for audio events. In *2017 IEEE international conference on acoustics, speech and signal processing (ICASSP)*, pp. 776–780. IEEE, 2017.
- Hayakawa, A., Ishii, M., Shibuya, T., and Mitsufuji, Y. Discriminator-guided cooperative diffusion for joint audio and video generation. *arXiv preprint arXiv:2405.17842*, 2024.
- Hershey, S., Ellis, D. P., Fonseca, E., Jansen, A., Liu, C., Moore, R. C., and Plakal, M. The benefit of temporally-strong labels in audio event classification. In *ICASSP 2021-2021 IEEE International Conference on Acoustics, Speech and Signal Processing (ICASSP)*, pp. 366–370. IEEE, 2021.
- Ho, J., Jain, A., and Abbeel, P. Denoising diffusion probabilistic models. *Advances in neural information processing systems*, 33:6840–6851, 2020.
- Iashin, V. and Rahtu, E. Taming visually guided sound generation. *arXiv preprint arXiv:2110.08791*, 2021.
- Jeong, Y., Ryoo, W., Lee, S., Seo, D., Byeon, W., Kim, S., and Kim, J. The power of sound (tpos): Audio reactive video generation with stable diffusion. In *Proceedings of the IEEE/CVF International Conference on Computer Vision*, pp. 7822–7832, 2023.
- Kong, J., Kim, J., and Bae, J. Hifi-gan: Generative adversarial networks for efficient and high fidelity speech synthesis. *Advances in neural information processing systems*, 33:17022–17033, 2020.
- Lee, S., Kong, C., Jeon, D., and Kwak, N. Aadiff: Audio-aligned video synthesis with text-to-image diffusion. *arXiv preprint arXiv:2305.04001*, 2023.
- Lee, S. H., Oh, G., Byeon, W., Kim, C., Ryoo, W. J., Yoon, S. H., Cho, H., Bae, J., Kim, J., and Kim, S. Sound-guided semantic video generation. In *European Conference on Computer Vision*, pp. 34–50. Springer, 2022.
- Li, Y., Zhang, C., Yu, G., Yang, W., Wang, Z., Fu, B., Lin, G., Shen, C., Chen, L., and Wei, Y. Enhanced visual instruction tuning with synthesized image-dialogue data. pp. 14512–14531, 2024. doi: 10.18653/v1/2024.findings-acl.864.
- Liu, H., Chen, Z., Yuan, Y., Mei, X., Liu, X., Mandic, D., Wang, W., and Plumbley, M. D. Audioldm: Text-to-audio generation with latent diffusion models. In *Proceedings of the 40th International Conference on Machine Learning*, volume 202, pp. 21450–21474, 2023.
- Liu, H., Yuan, Y., Liu, X., Mei, X., Kong, Q., Tian, Q., Wang, Y., Wang, W., Wang, Y., and Plumbley, M. D. Audioldm 2: Learning holistic audio generation with self-supervised pretraining. *IEEE/ACM Transactions on Audio, Speech, and Language Processing*, 32:2871–2883, 2024a. doi: 10.1109/TASLP.2024.3399607.
- Liu, X., Iqbal, T., Zhao, J., Huang, Q., Plumbley, M. D., and Wang, W. Conditional sound generation using neural discrete time-frequency representation learning. In *2021 IEEE 31st International Workshop on Machine Learning for Signal Processing (MLSP)*, pp. 1–6. IEEE, 2021.

- Liu, X., Su, K., and Shlizerman, E. Tell what you hear from what you see—video to audio generation through text. *arXiv preprint arXiv:2411.05679*, 2024b.
- Luo, S., Yan, C., Hu, C., and Zhao, H. Diff-foley: Synchronized video-to-audio synthesis with latent diffusion models. *Advances in Neural Information Processing Systems*, 36, 2024.
- Peebles, W. and Xie, S. Scalable diffusion models with transformers. In *Proceedings of the IEEE/CVF International Conference on Computer Vision*, pp. 4195–4205, 2023.
- Polyak, A., Zohar, A., Brown, A., Tjandra, A., Sinha, A., Lee, A., Vyas, A., Shi, B., Ma, C.-Y., Chuang, C.-Y., et al. Movie gen: A cast of media foundation models. *arXiv preprint arXiv:2410.13720*, 2024.
- Ramesh, A., Dhariwal, P., Nichol, A., Chu, C., and Chen, M. Hierarchical text-conditional image generation with clip latents. *arXiv preprint arXiv:2204.06125*, 1(2):3, 2022.
- Rombach, R., Blattmann, A., Lorenz, D., Esser, P., and Ommer, B. High-resolution image synthesis with latent diffusion models. In *Proceedings of the IEEE/CVF conference on computer vision and pattern recognition*, pp. 10684–10695, 2022.
- Ronneberger, O., Fischer, P., and Brox, T. U-net: Convolutional networks for biomedical image segmentation. In *Medical image computing and computer-assisted intervention—MICCAI 2015: 18th international conference, Munich, Germany, October 5-9, 2015, proceedings, part III 18*, pp. 234–241. Springer, 2015.
- Ruan, L., Ma, Y., Yang, H., He, H., Liu, B., Fu, J., Yuan, N. J., Jin, Q., and Guo, B. Mm-diffusion: Learning multi-modal diffusion models for joint audio and video generation. In *Proceedings of the IEEE/CVF Conference on Computer Vision and Pattern Recognition*, pp. 10219–10228, 2023.
- Song, Z., Wang, C., Sheng, J., Zhang, C., Yu, G., Fan, J., and Chen, T. MovieLLM: Enhancing long video understanding with ai-generated movies. *arXiv preprint arXiv:2403.01422*, 2024.
- Sun, M., Wang, W., Qiao, Y., Sun, J., Qin, Z., Guo, L., Zhu, X., and Liu, J. Mm-ldm: Multi-modal latent diffusion model for sounding video generation. In *Proceedings of the 32nd ACM International Conference on Multimedia*, pp. 10853–10861, 2024.
- Tan, X., Chen, J., Liu, H., Cong, J., Zhang, C., Liu, Y., Wang, X., Leng, Y., Yi, Y., He, L., Zhao, S., Qin, T., Soong, F., and Liu, T.-Y. Naturalspeech: End-to-end text-to-speech synthesis with human-level quality. *IEEE Transactions on Pattern Analysis and Machine Intelligence*, 46(6):4234–4245, 2024. doi: 10.1109/TPAMI.2024.3356232.
- Viertola, I., Iashin, V., and Rahtu, E. Temporally aligned audio for video with autoregression. *arXiv preprint arXiv:2409.13689*, 2024.
- Wang, K., Deng, S., Shi, J., Hatzinakos, D., and Tian, Y. Av-dit: Efficient audio-visual diffusion transformer for joint audio and video generation. *arXiv preprint arXiv:2406.07686*, 2024a.
- Wang, Y., Chen, M., and Li, X. Continuous emotion-based image-to-music generation. *IEEE Transactions on Multimedia*, 26:5670–5679, 2024b. doi: 10.1109/TMM.2023.3338089.
- Wang, Y., Chen, X., Ma, X., Zhou, S., Huang, Z., Wang, Y., Yang, C., He, Y., Yu, J., Yang, P., et al. Lavie: High-quality video generation with cascaded latent diffusion models. *International Journal of Computer Vision*, pp. 1–20, 2024c.
- Wang, Y., Guo, W., Huang, R., Huang, J., Wang, Z., You, F., Li, R., and Zhao, Z. Frieren: Efficient video-to-audio generation network with rectified flow matching. In *The Thirty-eighth Annual Conference on Neural Information Processing Systems*, 2024d. URL <https://openreview.net/forum?id=prXfM5X2Db>.
- Xing, Y., He, Y., Tian, Z., Wang, X., and Chen, Q. Seeing and hearing: Open-domain visual-audio generation with diffusion latent aligners. In *Proceedings of the IEEE/CVF Conference on Computer Vision and Pattern Recognition*, pp. 7151–7161, 2024.
- Xu, L., Zhao, Y., Zhou, D., Lin, Z., Ng, S. K., and Feng, J. Pllava: Parameter-free llava extension from images to videos for video dense captioning. *arXiv preprint arXiv:2404.16994*, 2024.
- Yariv, G., Gat, I., Benaim, S., Wolf, L., Schwartz, I., and Adi, Y. Diverse and aligned audio-to-video generation via text-to-video model adaptation. In *Proceedings of the AAAI Conference on Artificial Intelligence*, volume 38, pp. 6639–6647, 2024.
- Zhang, L., Mo, S., Zhang, Y., and Morgado, P. Audio-synchronized visual animation. In *European Conference on Computer Vision*, pp. 1–18. Springer, 2025.
- Zhang, Y., Gu, Y., Zeng, Y., Xing, Z., Wang, Y., Wu, Z., and Chen, K. FoleyCrafter: Bring silent videos to life with lifelike and synchronized sounds. *arXiv preprint arXiv:2407.01494*, 2024.

Zheng, Z., Peng, X., Yang, T., Shen, C., Li, S., Liu, H., Zhou, Y., Li, T., and You, Y. Open-sora: Democratizing efficient video production for all. *arXiv preprint arXiv:2412.20404*, 2024.

Zhu, J., Gao, L., Song, J., Li, Y.-F., Zheng, F., Li, X., and Shen, H. T. Label-guided generative adversarial network for realistic image synthesis. *IEEE Transactions on Pattern Analysis and Machine Intelligence*, 45(3):3311–3328, 2023. doi: 10.1109/TPAMI.2022.3186752.